Responsive mechanism of three novel hypochlorous acid fluorescent probes and solvent effect on their sensing performance*

Yong Zhou(周勇)[1], Yun-Kun Wang(王云坤)[1], Xiao-Fei Wang(王晓菲)[1], Yu-Jin Zhang(张玉瑾)[2], and Chuan-Kui Wang(王传奎)[1,†]

[1] *Shandong Provincial Key Laboratory of Medical Physics and Image Processing Technology, School of Physics and Electronics, Shandong Normal University, Jinan* 250358, *China*

[2] *School of Science, Qilu University of Technology, Jinan* 250353, *China*

(Received 21 March 2017; revised manuscript received 5 May 2017; published online 10 July 2017)

Optical properties and responsive mechanisms of three newly synthesized fluorescent probes for hypochlorous acid (HOCl) are investigated by employing time-dependent density functional theory. The computational results show that the absorption and emission properties of these probes change obviously when they react with hypochlorous acid. It is found that the probe FHZ has the best performance according to the probing behavior. Moreover, the responsive mechanisms of the probes are studied by analyzing the distributions of molecular orbitals and charge transfer, which are shown as the photon-induced electron transfer (PET) for FHZ and the intramolecular charge transfer (ICT) for the other two probes. Specially, solvent effect on optical properties of the probe FHZ before and after reaction is studied within the polarizable continuum model (PCM). It is shown that performance of the probe depends crucially on the solvent polarity. Our computational results agree well with the experimental measurement, and provide information for design of efficient two-photon fluorescent probes.

Keywords: responsive mechanism, hypochlorous acid fluorescentprobe, solvent effect, two-photon absorption

PACS: 31.15.A–, 31.70.Dk, 33.80.Wz **DOI:** 10.1088/1674-1056/26/8/083102

1. Introduction

Hypochlorous acid (HOCl), a weak unstable acid known only in solution and in its salts, is an extremely potent oxidant, widely known as a "killer" for pathogenic bacteria in the innate immune system.[1] Meanwhile, intracellular HOCl plays significant roles in regulating inflammation and cellular apoptosis, such as permeabilization in chondriosome[2] and breakdown in lysosome.[3] Due to the low concentration, strong oxidization, and short life time of HOCl, it is quite difficult to investigate intracellular HOCl directly. Therefore, lots of attention have been paid on studying the mechanism of the action of HOCl in the living organisms recently.[4,5] Fluorescent probes have attracted much attention owing to their highly sensitivity, good selectivity and fast response, they have been recognized as one of the most powerful tools to monitor and visualize molecules in chemical, biological, and environmental applications.[6,7] Due to these outstanding advantages, fluorescent probe is an ideal tool to detect HOCl. Actually, many fluorescent probes have been synthesized in the past few years.[8–14]

Recently, Lin *et al.*[15] synthesized the first two-photon fluorescent probe for HOCl. Its mitochondria and lysosome targetable derivatives were successfully applied to detect intracellular HOCl in corresponding organelles. These probes exhibit second level response, good selectivity, and nanomole level sensitivity toward HOCl. Cell imaging experiments indicate these probes display good cell penetration and localize in living cells. In particular, imaging of macrophage cells during inflammation conditions in a murine model also obtained within two-photon excitation. They own a acedan as two-photon fluorophore which has a typical "push–pull"structure. Excited at 375 nm, the fluorescence intensity of these probes at 500 nm increased more than 600-fold when 20 equiv of HOCl was added, which results from the recovery of "push-pull" structure when the oxathiolane was deprotected by HOCl. Zhang *et al.*[16] developed a novel HOCl fluorescent probe in green emissions, providing the real-time discrimination and quantitative analysis of the HOCl in living organisms. This probe is constructed by introducing a rhodamine derivatives as a fluorophore and grafting an additional five-membered heterocyclic ring and a lateral triethylene glycol chain to a fluorescein mother, which turn off the fluorescence of fluorescein. It emits markable green fluorescence at 520 nm excited at its absorption maximum of 490 nm, while its fluorescein-hydrazine derivative is nonfluorescent. The probe exhibits a series of remarkable features: the rapid, sensitive, and dynamic responses; the high biocompatibility of passing through various biological barriers into cells, blood, organs, and tissues. On the basis of these advantages, the distributions of spontaneous HOCl in the organs of a normal-state zebrafish are

* Project supported by the National Natural Science Foundation of China (Grant Nos. 11374195 and 11404193) and the Taishan Scholar Program of Shandong Province, China.

† Corresponding author. E-mail: ckwang@sdnu.edu.cn

© 2017 Chinese Physical Society and IOP Publishing Ltd

clearly revealed by the accumulation of probes there. Therefore, the HOCl fluorescent probes synthesized by two experimental groups are powerful tools in investigations of HOCl at subcellular and tissue levels.

Even though they have several desirable features in the experiment, theoretical analysis of the probes are not given, and responsive mechanism is not pointed out in the experimental reports. Moreover, sensing performances of the probes in different solvents are not discussed. Therefore, in this paper, we employ the density functional and response theory to describe properties of these probes. Based on the same theoretical method, we calculate optical properties of six molecules in water, including the one-photon absorption (OPA), two-photon absorption (TPA), and the emission properties. All of our computational results are in reasonable agreement with the experimental ones. Among these compounds, the most promising fluorescent probe is selected. In addition, solvent effect is investigated within the polarizable continuum model (PCM). Our study is helpful for understanding responsive mechanism of the fluorescent probes and the solvent influence.

2. Theoretical method and computational details

The expression of transition probability of one-photon absorption and emission between the ground state $|g\rangle$ and the excited state is given by the oscillator strength[17]

$$f_{kg} = \frac{2\omega_{kg}}{3}\sum_i \left|\mu_i^{kg}\right|^2, \tag{1}$$

Where ω_{kg} is excited energy of the state $|k\rangle$ and μ_i is the electric dipole moment operator in the direction, the summation is performed over the molecular x, y, and z axes.

The TPA cross-section that can be directly compared with the experimental results is defined as[18]

$$\sigma_{\rm tp} = \frac{4\pi^2 a_0^5 \alpha}{15c}\frac{\omega^2}{\Gamma_{\rm f}}\frac{g(\omega)}{n^2}\delta_{\rm tp}, \tag{2}$$

where a_0 donates the Bohr radius, c is the speed of light, α is the fine structure constant, ω is the photon frequency of the incident light, and $g(\omega)$ denotes the spectrum line profile, which is assumed to be a δ function here and $\Gamma_{\rm f}$ is the lifetime broadening of the final state, which is commonly assumed to be 0.1 eV.[19] $\delta_{\rm tp}$ is the orientation average value of the two-photon absorption probability[20,21]

$$\delta_{\rm tp} = \sum_{\alpha\beta}[F\times S_{\alpha\alpha}\times S^*_{\beta\beta} + G\times S_{\alpha\beta}\times S^*_{\alpha\beta} + H\times S_{\alpha\beta}\times S^*_{\beta\alpha}], \tag{3}$$

where F, G, and H are coefficients depending on the polarization of the light. For the linearly polarized light, F, G, and H are 2, 2, 2, and for the circular case, they are -2, 3, 3. In the present letter, we only consider the case excited by a linearly polarized monochromatic beam. $S_{\alpha\beta}$ is the two-photon transition matrix element. For the absorption of two photons with the frequence ω_f, it can be written as[17]

$$S_{\alpha\beta} = \frac{1}{2\hbar}\sum_n\left[\frac{\langle 0|\,\hat{\mu}_\alpha\,|n\rangle\langle n|\,\hat{\mu}_\beta\,|f\rangle}{\omega_{n0}-\omega_1} + \frac{\langle 0|\,\hat{\mu}_\beta\,|n\rangle\langle n|\,\hat{\mu}_\alpha\,|f\rangle}{\omega_{n0}-\omega_2}\right], \tag{4}$$

where ω_{n0} and ω_1 denote the excitation frequency of the intermediate state $|n\rangle$ and final state $|f\rangle$ respectively, $\alpha,\beta\in\{x,y,z\}$. And the summation goes over all of the intermediate states including the ground state $|0\rangle$ and the final state $|f\rangle$.

In this work, geometries of the studied molecules are fully optimized at the time-dependent hybrid density functional theory (TDDFT)/Becke's three parametrized Lee–Yang–Parr (B3LYP) level in Gaussian09 package.[22] Frequency calculations are performed to verify the stabilities of the optimized structures at the same level. All calculations are implemented in the Gaussian09 software package except for TPA properties that are obtained in Dalton2013 package.[23] The basis set 6-31G(d) is chosen for all studies. Furthermore, solvent effect is taken into account within the polarizable continuum model (PCM).

3. Results and discussion

3.1. Molecular structure

The researched molecular geometry is presented in Fig. 1. For briefness, in the present article, the first mitochondria and lysosome targetable HOCl two-photon fluorescent probes[15] are named as Mol. 1 and Mol. 2, and their products with hypochlorous acid are respectively labeled as Mol. 1+ and Mol. 2+. It is expected that Mol. 1 & Mol. 2 are nonfluorescent due to break of the "push-pull" structure. However, the reaction with HOCl, which unprotects the oxathiolane group to reveal the ketone, would lead to fluorescence recovery. The second kind of probe is labeled as the same name FHZ as one given in the experiment.[16] The fluorescein-hydrazine derivative FHZ is nonfluorescent due to the disruption of conjugated system of fluorophore and the decrease of electron delocalization induced by the newly formed five-membered ring.

Based on the fully optimized geometry, frontier orbital energies and energy gap ($\Delta E_{\rm H-L}$) between the highest occupied molecular orbital (HOMO) and the lowest unoccupied molecular orbital (LUMO) are schematically shown in Fig. 2. For the molecule Mol. 1+ (Mol. 2+), their HOMO and LUMO energies move down compared with those of Mol. 1 (Mol. 2). It is noteworthy that the unoccupied molecular orbital of Mol. 1 (Mol. 1+) is more compacter than Mol. 2 (Mol. 2+). This can be attributed to their difference of terminal

group. When FHZ reacting with hypochlorous acid, the energy of HOMO goes up and the energy of LUMO goes down, leading to the narrower energy gap, which seems to make the absorption process more likely to happen.

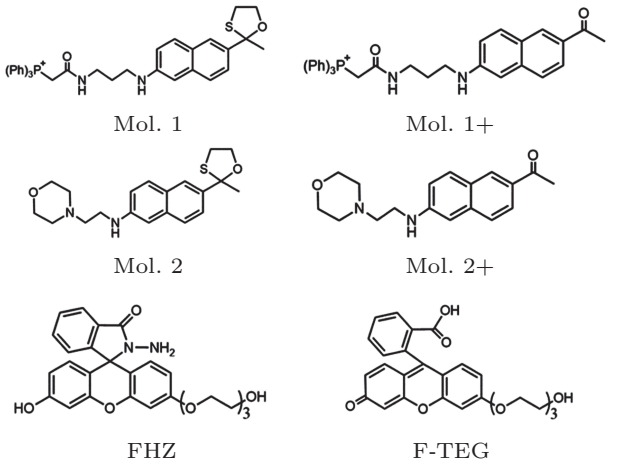


Fig. 1. The geometric structure of compounds.

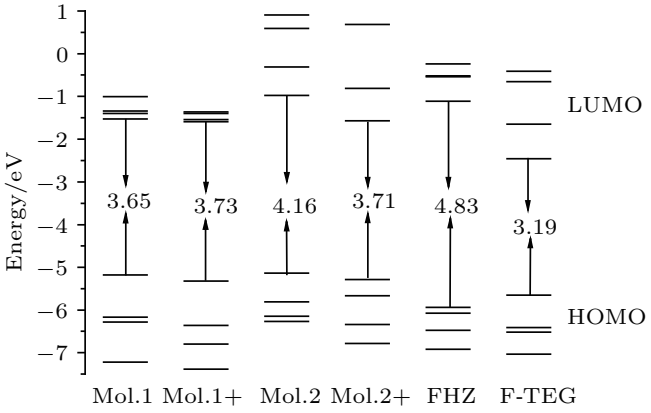


Fig. 2. Frontier orbital energies of the compounds.

3.2. One-photon absorption

Considering the fluorescent probe mainly works in living cells and tissues that mostly composed of water, we thus investigate properties of the probes under water solvent. The OPA properties of the compounds, including excitation energy, the corresponding OPA wavelengths, oscillator strengths, and transition features are calculated. Only the states with the largest oscillator strengths in the first five excited states are listed. As shown in Table 1, absorption peaks of the compounds Mol. 1 and Mol. 2 are located at 338 nm and 293 nm. When they react with HOCl, Mol. 1+ shows an absorption peak at 366 nm with oscillator strength of 0.43, and Mol. 2+ shows an absorption peak locating at 367 nm with oscillator strength of 0.42. We can see that computational wavelengths of both Mol. 1+ and Mol. 2+ agree well with the experimental value of 375 nm. The maximum OPA peak of Mol. 1 (Mol. 2) shows a redshift feature upon combing with HOCl, which is well consistent with the experimental result in trend.

Table 1. One-photon absorption (OPA) properties in H_2O, including the excitation energy E_{opa} (eV), the corresponding wavelength λ_{opa} (nm), the oscillator strength δ_{opa} (a.u.) and transition feature. H (L) denotes the HOMO (LUMO).

Mol.	E_{opa}/eV	λ_{opa}/nm	λ^{a}_{opa}/nm	δ_{opa}/a.u.	Transition feature	
Mol. 1	3.67	338		0.10	H→L+3	91.6%
Mol. 1+	3.39	366	375[a]	0.43	H→L	95.8%
Mol. 2	4.24	293		0.22	H→L+1	70.1%
Mol. 2+	3.38	367	375[a]	0.42	H→L	95.7%
FHZ	5.28	235		0.26	H→L+2	38.5%
					H→L+1	31.8%
F-TEG	2.98	416	488[a]	0.43	H→L	73.5%

[a] Experimental results taken from Refs. [15] and [16].

Table 1 also shows that absorption peak of the compound. FHZ is located at 235 nm with oscillator strength of 0.26, which mainly originates from HOMO to LUMO+1 and HOMO to LUMO+2. When reacting with HOCl, the product F-TEG shows an absorption peak at 416 nm with oscillator strength of 0.43. This discrepancy with the experimental wavelength of 488 nm may result from a few factors, such as the vibrational contribution, the interaction between laser and molecules.

3.3. Two-photon absorption

The two-photon absorption properties including excitation energies, the corresponding two-photon wavelengths, and cross sections of the lowest five excited states are listed in Table 2. As shown in Table 2, the largest TPA cross section of compounds Mol. 1, Mol. 2, and FHZ are 46 GM, (1 GM = 10^{-50} cm^4·s/photon), 99 GM, and 49 GM, respectively, showing an order of Mol. 2 > FHZ > Mol. 1. When they react with hypochlorous acid, the respective values are 75 GM, 99 GM, and 659 GM, showing an order of F-TEG > Mol. 2+ > Mol. 1+. It is observed that the TPA cross section of the probe F-TEG is significantly enhanced compared with that of the probe FHZ, demonstrating the preferred performance of this probe.

3.4. Fluorescent emission

According to the Kasha's rule, the fluorescence occurs in appreciable yield only from the first excited state to ground state. Based on the fully optimized first excited state geometries of the compounds, emission properties of these probes and products, including emission energies, the corresponding emission wavelengths, oscillator strengths, transition features, and fluorescent lifetime in water are listed in Table 3. The fluorescent lifetime is calculated by the Einstein theory of radiation (in unit a.u.),

$$\tau = c^3/(2E_{flu}^2\delta_{ope}). \quad (5)$$

The emission peaks for the compounds Mol. 1, Mol. 2, and FHZ are located at 624 nm, 404 nm, and 1241 nm with

Table 2. Two-photon absorption (TPA) properties of the compounds in H_2O, including the excitation energy E_{tpa} (eV), the corresponding two-photon wavelength λ_{tpa} (nm), and the TPA cross section σ_{tpa} (GM = 10^{-50} cm^4·s/photon) of the five lowest excited states.

Mol	E_{tpa}/eV	λ_{tpa}/nm	σ_{tpa}/GM	Mol	E_{tpa}/eV	λ_{tpa}/nm	σ_{tpa}/GM
Mol. 1	3.34	742	0	Mol. 1+	3.39	731	25
	3.52	704	4		3.46	717	5
	3.56	696	0		3.65	680	75
						750[a]	83[a]
	3.67	676	0		3.69	672	16
	4.00	620	46		3.81	652	6
Mol. 2	3.65	679	10	Mol. 2+	3.38	824	13
	4.24	585	0		3.73	665	99
						750[a]	74[a]
	4.42	561	99		3.80	653	19
	4.63	535	4		3.83	647	0
	4.79	517	27		4.40	563	5
FHZ	4.17	595	1	F-TEG	2.97	833	659
	4.36	569	1		2.98	831	65
	4.66	532	0		3.41	727	55
	4.70	527	49		3.48	712	14
	4.77	520	2		4.09	606	200

[a] Experimental results taken from Refs. [15] and [16].

Table 3. Fluorescent emission properties of the compounds in H_2O, including the emission energy E_{flu} (eV), the corresponding emission wavelength λ_{ope} (nm), the oscillator strength δ_{ope} (a.u.) and fluorescent lifetime τ (ns).

Mol	E_{flu}/eV	λ_{ope}/nm	λ^{a}_{ope}/nm	δ_{ope}/a.u.	Transition feature	τ/ns
Mol. 1	1.99	624		0.00	H→L 99.4%	
Mol. 1+	2.96	419	500[a]	0.56	H→L 98.7%	4.70
Mol. 2	3.07	404		0.20	H→L 98.0%	12.24
Mol. 2+	2.51	495	500[a]	0.35	H→L 99.2%	10.46
FHZ	1.00	1241		0.00	H→L 99.5%	
F-TEG	2.32	535	520[a]	0.56	H→L 96.2%	7.66

[a] Experimental results taken from Refs. [15] and [16].

small oscillator strengthes of 0.00, 0.20, and 0.00, respectively. These results are consistent with the experimental measurement. After reaction with HOCl, the emission intensity of Mol. 1+, Mol. 2+, and F-TEG are highly enlarged to 0.56, 0.35, 0.56, and the emission wavelengths are located at 419 nm, 495 nm, and 535 nm. Upon addition of HOCl, fluorescence enhancement is observed for all three fluorescent probes, and the wavelength of Mol. 2 shows redshift, which is in the same trend as the available experimental results.

Fluorescent lifetime is also an important factor for evaluating the probes. After reaction, Mol. 1+ has the shortest emission lifetime of 4.70 ns, followed by F-TEG with emission lifetime of 7.66 ns and Mol. 2+ with emission lifetime of 10.46 ns. The shorter fluorescent lifetime means stronger emission intensity, while the too short fluorescent lifetime is easy to cause the interference of excitation light. Therefore, fluorescent probes with moderate fluorescent lifetime are the best choice. Overall, we can make such a conclusion that FHZ is the most suitable probe for detecting HOCl among the three probes.

3.5. Responsive mechanism

The charge population of the fluorophore is of great importance for deciding their optical properties. Thus, we analyze the mulliken population of the molecules Mol. 1 (Mol. 2) and Mol. 1+ (Mol. 2+). To obtain a clear view, these compounds are separated into three parts as shown in Fig. 3, in which part A is the terminal group of these molecules, parts B is the donor, and part C is acceptor. The charges of different parts are given in Table 4. We can see that when Mol. 1 combines with HOCl, Q_C is enlarged from $-0.073e$ to $-0.118e$, and for compound Mol. 2, Q_C is enlarged from $-0.075e$ to $-0.119e$. It is demonstrated that electron push–pull capabilities of these molecules are increased when they react with HOCl.

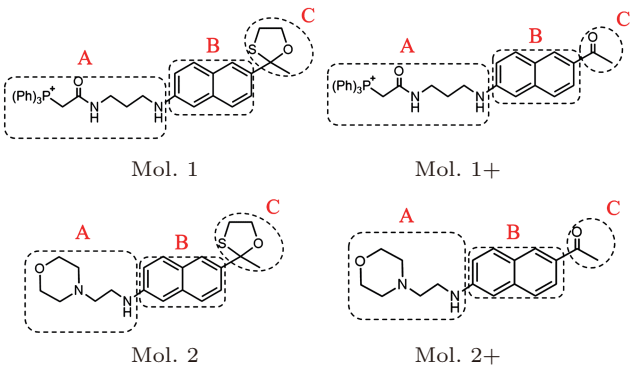


Fig. 3. (color online) Molecules are divided into A, B, and C parts.

Table 4. The Mulliken charge (e) of different parts of the molecules.

Mol	Q_A/e	Q_B/e	Q_C/e
Mol. 1	0.855	0.218	−0.073
Mol. 1+	0.877	0.241	−0.118
Mol. 2	−0.145	0.220	−0.075
Mol. 2+	−0.123	0.241	−0.119

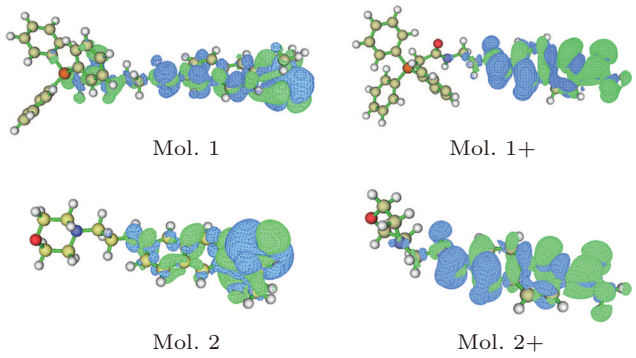


Fig. 4. (color online) The charge transfer between the excited state and the ground state. The blue and green areas represent electron loss and gain, respectively.

To figure out the electronic charge transfer of molecules Mol. 1 (Mol. 2) and Mol. 1+ (Mol. 2+) intuitively, we show the charge transfer between the ground state and the excited state in Fig. 4 drawn by the Multiwfn.[24,25] This method has been proved to be an available and useful way.[26] It is demonstrated that the charge transfer process has a considerable variation after adding HOCl. Taking Mol. 1 as an example, we can see that the blue and green areas show feature of overlapping in general, which means that the charge transfer is not obvious. After reacting with HOCl, the blue areas and green areas of Mol. 1+ show a clear separation, which indicates that an obvious charge transfer takes place. We thus point out that the responsive mechanism of the probes is attributed to the intramolecular charge transfer (ICT) process.

We further discuss responsive mechanism of the probe FHZ. According to the general characteristic of the probe, one would predict that there probably exist electron transfer between receptor and fluorophore as the compounds are excited. This process can be investigated by analysis of molecular orbital distribution diagram, which has been proved to be a useful way.[27] Molecular orbitals can be classified in view of fluorophore and receptor. Therefore, we pick out the orbitals which mainly locate in the part of fluorophore and receptor shown in the left and right column in Fig. 5.

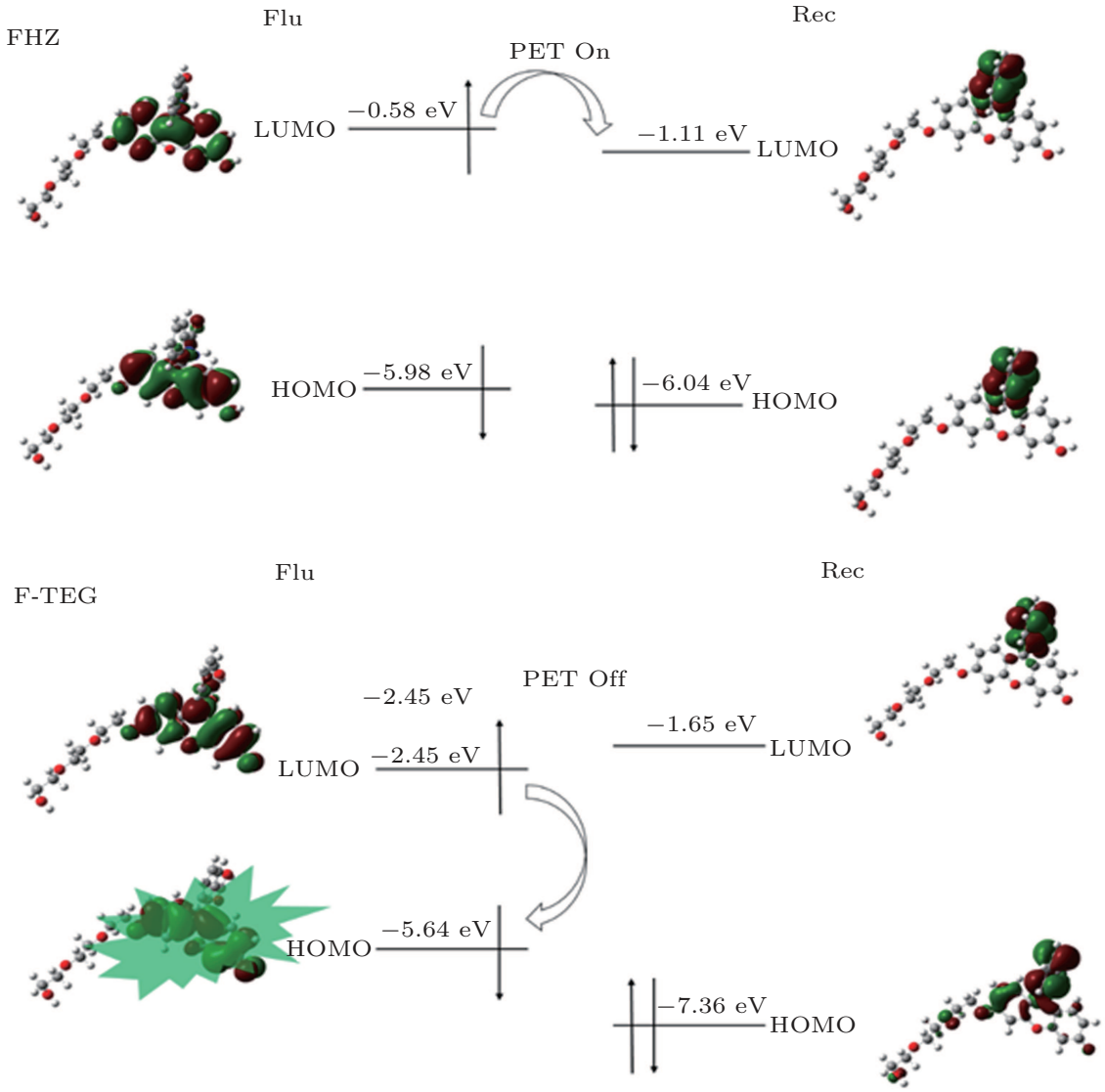


Fig. 5. (color online) The PET (photo-induced electron transfer) process of molecules FHZ and F-TEG.

The HOMO and LUMO energies of the fluorophore for FHZ in Fig. 5 are respectively −5.98 eV and −0.58 eV, while the energies of receptor are respectively −6.04 eV and −1.11 eV. As shown in Fig. 5, the electron transfer from the fluorescence group to the recognition group takes place because the LUMO of recognition group is lower than that of the fluorescence group. As a result, the excited electron can not return to the ground state, leading to quenching of fluorescence. However, when FHZ reacts with HOCl to be the product F-TEG, as shown in Fig. 5, the LUMO energy of the fluorophore sharply moves down to −2.45 eV while the LUMO energy of the receptors lightly moves down to −1.65 eV. Therefore, electron transfer process between the fluorophore and receptor can not occur because the LUMO of the fluorophore is lower than that of receptor. Thus, remarkable fluorescence can be observed. The responsive mechanism of the probe is attributed to photoinduced electron transfer (PET) process.

3.6. The solvent effect on FHZ and F-TEG

To investigate the influence of solvent on probe FHZ and its product F-TEG, we calculate the OPA features of FHZ and F-TEG in vacuum, benzene, acetone, methanol, water, which are shown in Table 5. Only results of the excited states with oscillator strengths $\delta_{opa} > 0.1$ are displayed. The polarity of benzene, acetone, methanol, and water are 3.0, 5.4, 6.6, and 10.2, respectively. As can be seen from Table 5, after reacting with HOCl, the OPA peak of F-TEG appears redshift and the oscillator strength gradually increases compared with FHZ in all solvent.

Table 5. One-photon absorption properties (OPA) in vacuum, benzene, acetone, MeOH, H_2O including the excitation energy E_{opa} (eV), the corresponding wavelength λ_{opa} (nm), the oscillator strength δ_{opa} (a.u.), and transition feature.

Solvent	Mol.	E_{opa}/eV	λ_{opa}/nm	δ_{opa}/a.u.	Transition feature	
Vacuum	FHZ	5.18	240	0.17	H-1→L+4	24.2%
	F-TEG	3.61	344	0.25	H-2→L	81.7%
Benzene	FHZ	5.15	241	0.26	H-6→L	19.2%
					H-3→L	19.2%
	F-TEG	2.93	423	0.51	H→L	90.2%
Acetone	FHZ	5.28	235	0.25	H→L+4	33.0%
	F-TEG	2.98	417	0.52	H→L	88.3%
MeOH	FHZ	5.29	235	0.37	H-2→L+2	32.4%
	F-TEG	2.98	428	0.51	H→L	86.9%
H_2O	FHZ	5.28	235	0.26	H→L+2	38.5%
					H→L+1	31.8%
	F-TEG	2.97	416	0.43	H→L	73.5%

TPA properties are further calculated as shown in Table 6. One can see that the TPA cross sections of compounds FHZ in vacuum, benzene, acetone, methanol, and water are 3 GM, 4 GM, 4 GM, 11 GM, and 49 GM, respectively. While reacting with HOCl, those are respectively 13 GM, 25 GM, 24 GM, 118 GM, and 659 GM in vacuum, benzene, acetone, methanol, and water. With the increase of polarity of the solution, the TPA cross section is enlarged gradually. As a consequence, the probe is more suitable for using in water to detect HOCl.

Table 6. Two-photon absorption (TPA) properties in vacuum, benzene, acetone, MeOH, H_2O, including the excitation energy E_{tpa} (eV), the corresponding two-photon wavelength λ_{tpa} (nm), and the TPA cross section σ_{tpa} (GM = 10^{-50} cm^4·s/photon) around the wavelength as twice times as one-photon excitation.

Solvent	Mol.	E_{tpa}/eV	λ_{tpa}/nm	σ_{tpa}/GM	Mol.	E_{tpa}/eV	λ_{tpa}/nm	σ_{tpa}/GM
Vacuum	FHZ	4.59	540	0	F-TEG	3.05	812	1
		4.71	526	1		3.61	687	13
		4.90	506	2		3.65	679	1
		5.00	496	1		3.94	630	1
		5.18	479	3		3.98	623	0
Benzene	FHZ	4.65	533	0	F-TEG	2.80	884	0
		4.74	524	1		2.93	847	4
		4.90	506	2		3.17	782	0
		4.92	504	4		3.52	704	25
		4.99	497	2		3.94	629	0
Acetone	FHZ	4.66	532	0	F-TEG	2.98	833	4
		4.70	528	1		3.38	733	0
		4.77	520	2		3.49	711	24
		4.95	501	4		4.12	602	0
		5.01	494	2		4.25	584	2
MeOH	FHZ	4.65	533	0	F-TEG	2.97	836	9
		4.80	517	2		2.98	832	0
		4.88	509	0		3.40	730	3
		4.94	502	11		3.49	711	48
		5.05	492	6		4.11	604	118
H_2O	FHZ	4.17	595	1	F-TEG	2.97	833	659
		4.36	569	1		2.98	831	65
		4.66	532	0		3.41	727	55
		4.70	527	49		3.48	712	14
		4.77	520	2		4.09	606	200

Based on the fully optimized first excited state structures of the compounds, emission properties of FHZ and F-TEG in vacuum, benzene, acetone, methanol, water are shown in Table 7. Computational emission intensity is changed remarkably in different solvent. One can see that in vacuum and benzene, where their polarities are quite small, the product F-TEGis non-fluorescent. As the increase of solvent polarity, the emission oscillator strengths are enlarged, namely, F-TEG becomes fluorescent. As a conclusion, whether the probe can be used or not is sensive to the solution environment.

Table 7. Fluorescent emission properties in vacuum, benzene, acetone, MeOH, H_2O, including the emission energy E_{flu} (eV), the corresponding emission wavelength λ_{ope} (nm), the oscillator strength δ_{ope} (a.u.), and fluorescent lifetime τ (ns).

Solvent	Mol.	E_{flu}/eV	λ_{ope}/nm	δ_{ope}/a.u.	Transition feature	τ/ns
Vacuum	FHZ	0.59	2101	0.00	H→L 99.7%	
	F-TEG	1.95	637	0.00	H→L 99.5%	
Benzene	FHZ	0.77	1615	0.00	H→L 99.6%	
	F-TEG	2.10	589	0.00	H→L 97.6%	
Acetone	FHZ	0.97	1275	0.00	H→L 99.5%	
	F-TEG	2.31	537	0.51	H→L 95.7%	8.48
MeOH	FHZ	0.98	1262	0.00	H→L 99.5%	
	F-TEG	2.31	536	0.53	H→L 96.0%	8.16
H_2O	FHZ	1.00	1241	0.00	H→L 99.5%	
	F-TEG	2.32	535	0.56	H→L 96.2%	7.66

4. Conclusion

In summary, three probes for sensing hypochlorous acid synthesized by two experimental groups are investigated at the same theoretical level, which provides opportunity for one to compare their performance directy. The optical properties including OPA, TPA, and emission properties of the probes and their producs with hypochlorous acid are obtained. The probe FHZ is demonstrated to have the best behavior. The responsive mechanisms of the probes are analyzed, which are ICT for Mol. 1 (Mol. 2) and PET for FHZ. Furthermore, it is shown that solvent has an obvious effect on performance of the probe FHZ, moreover, the probe is inapplicable in solvent with weak polarity. This study provides a theoretical explanation of the experimental results.

References

[1] Winterbourn C C, Hampton M B, Livesey J H and Kettle A J 2006 *J. Biol. Chem.* **281** 39860
[2] Yang Y T, Whiteman M and Gieseg S P 2012 *Biochim. Biophys. Acta* **1823** 420
[3] Yap Y W, Whiteman M, Bay B H, Li Y, Sheu F S, Qi R Z, Tan C H and Cheung N S 2006 *J. Neurosci.* **98** 1597
[4] Marnett L J 2012 *J. Org. Chem.* **77** 5224
[5] Rees M D, Hawkins C L and Davies M J 2003 *J. Am. Chem. Soc.* **125** 13719
[6] Yang W J, Zhang Y J and Wang C K 2015 *Acta Phys. Chim. Sin.* **31** 2303
[7] Zhang YJ, Wang X, Zhou Y and Wang C K 2016 *Chem. Phys. Lett.* **658** 125
[8] Chen W C, Venkatesan P and Wu S P 2015 *Anal. Chim. Acta* **882** 68
[9] Cheng X, Jia H, Long T, Feng J, Qin J and Li Z 2011 *Chem. Commun.* **47** 11978
[10] Li H, Guan L, Zhang X, Yu H, Huang D, Sun M and Wang S 2016 *Talanta* **161** 592
[11] Venkatesan P and Wu S P 2015 *Analyst* **140** 1349
[12] Xu Q, Lee K A, Lee S, Lee K M, Lee W J and Yoon J 2013 *J. Am. Chem. Soc.* **135** 9944
[13] Yang Y K, Cho H J, Lee J, Shin I and Tae J 2009 *Org. Lett.* **11** 859
[14] Zhou X H, Jiang Y R, Zhao X J and Guo D 2016 *Talanta* **160** 470
[15] Yuan L, Wang L, Agrawalla B K, Park S J, Zhu H, Sivaraman B, Peng J, Xu Q H and Chang Y T 2015 *J. Am. Chem. Soc.* **137** 5930
[16] Zhang R, Zhao J, Han G, Liu Z, Liu C, Zhang C, Liu B, Jiang C, Liu R, Zhao T, Han M Y and Zhang Z 2016 *J. Am. Chem. Soc.* **138** 3769
[17] Sun Y H, Li J, Zhao K and Wang C K 2010 *Chin. Phys. B* **19** 044207
[18] Sun Y H and Wang C K 2011 *Chin. Phys. B* **20** 104204
[19] Albota M, Beljonne D, Bredas J L, Ehrlich J E, Fu J Y, Heikal A A, Hess S E, Kogej T, Levin M D, Marder S R, McCord-Maughon D, Perry J W, Rockel H, Rumi M, Subramaniam G, Webb W W, Wu X L and Xu C 1998 *Science* **281** 1653
[20] Monson P R and McClain W M 1970 *J. Chem. Phys.* **53** 29
[21] Luo Y, Norman P, Macak P and Ågren H 2000 *J. Phys. Chem. A* **104** 4718
[22] GAUSSIAN 09, References in http://www.gaussian.com/
[23] DALTON 2011 A Molecular Electronic Structure Program, Release Dalton2011, see http://daltonprogram.org/
[24] Lu T and Chen F 2012 *J. Comput. Chem.* **33** 580
[25] Lu T and Chen F W 2012 *J. Mol. Graph. Model. NLM.* **38** 314
[26] Zhang Y J, Zhang Q Y, Ding H J, Song X N and Wang C K 2015 *Chin. Phys. B* **24** 023301
[27] Zhang Y J, Yang W J and Wang C K 2016 *Chem. Phys.* **468** 37